Europace (2014) **16**, iv30–iv38
doi:10.1093/europace/euu230

In-silico assessment of the dynamic effects of amiodarone and dronedarone on human atrial patho-electrophysiology

Axel Loewe[1]*, Yannick Lutz[1], Mathias Wilhelms[1], Daniel Sinnecker[2], Petra Barthel[2], Eberhard P. Scholz[3], Olaf Dössel[1], Georg Schmidt[2,4], and Gunnar Seemann[1]

[1]Institute of Biomedical Engineering, Karlsruhe Institute of Technology (KIT), Kaiserstr. 12, 76128 Karlsruhe, Germany; [2]Department of Internal Medicine I—Klinikum rechts der Isar, Technische Universität München, 80636 München, Germany; [3]Department of Internal Medicine III, University Hospital Heidelberg, 69120 Heidelberg, Germany; and [4]DZHK (German Center for Cardiovascular Research) partner site Munich Heart Alliance, Munich, Germany

Received 30 July 2014; accepted after revision 2 August 2014

Aims The clinical efficacy in preventing the recurrence of atrial fibrillation (AF) is higher for amiodarone than for dronedarone. Moreover, pharmacotherapy with these drugs is less successful in patients with remodelled substrate induced by chronic AF (cAF) and patients suffering from familial AF. To date, the reasons for these phenomena are only incompletely understood. We analyse the effects of the drugs in a computational model of atrial electrophysiology.

Methods and results The Courtemanche–Ramirez–Nattel model was adapted to represent cAF remodelled tissue and hERG mutations N588K and L532P. The pharmacodynamics of amiodarone and dronedarone were investigated with respect to their dose and heart rate dependence by evaluating 10 descriptors of action potential morphology and conduction properties. An arrhythmia score was computed based on a subset of these biomarkers and analysed regarding circadian variation of drug concentration and heart rate. Action potential alternans at high frequencies was observed over the whole dronedarone concentration range at high frequencies, while amiodarone caused alternans only in a narrow range. The total score of dronedarone reached critical values in most of the investigated dynamic scenarios, while amiodarone caused only minor score oscillations. Compared with the other substrates, cAF showed significantly different characteristics resulting in a lower amiodarone but higher dronedarone concentration yielding the lowest score.

Conclusion Significant differences exist in the frequency and concentration-dependent effects between amiodarone and dronedarone and between different atrial substrates. Our results provide possible explanations for the superior efficacy of amiodarone and may aid in the design of substrate-specific pharmacotherapy for AF.

Keywords Mathematical model • Atrial fibrillation • Drug safety • Amiodarone • Dronedarone

Introduction

Atrial fibrillation (AF) is a relevant arrhythmia due to its high prevalence[1] and association with severe complications such as stroke, making efficient AF prevention and therapy a major clinical challenge. In patients with chronic AF (cAF), a long-term adaptation of the substrate known as atrial 'remodeling' promotes the maintenance of and susceptibility to AF ('AF begets AF').[1] Moreover, an increased susceptibility to AF is observed in patients with various gene mutations ('familial AF').[2]

Atrial fibrillation is treated with various antiarrhythmic drugs, such as amiodarone and dronedarone.[3] Due to their effective inhibition of potassium currents, both drugs are usually classified primarily as Class III agents, even though both drugs exert effects on multiple ion channels. Dronedarone is a derivative of amiodarone which was designed to reduce tissue accumulation and adverse side effects such as thyroid toxicity.[4] Besides certain differences in the inhibitory effects on ion channels, both drugs differ markedly in their pharmacokinetic properties: Amiodarone has a biological half-life of several weeks, caused mainly by accumulation in a third

* Corresponding author. Tel: +49 721 608 42790; fax: +49 721 608 42789. *E-mail address*: publications@ibt.kit.edu

What's new?

- Action potential alternans as a potential proarrhythmic mechanism was observed for a wide range of dronedarone concentrations but only a narrow range of amiodarone concentrations.
- Considering relevant drug concentration and heart rate variations, a newly proposed arrhythmia score peaks to critical values for dronedarone but not for amiodarone.
- In a remodelled substrate due to chronic atrial fibrillation (cAF), the effect of amiodarone and dronedarone differs significantly. Compared with a healthy substrate, the best score was obtained using a lower amiodarone but a higher dronedarone concentration.
- In contrast to the other substrates, cAF yielded worse scores for increased heart rates considering relevant concentrations of both drugs.

compartment due to its lipophilic properties. In contrast, dronedarone is less lipophilic and has a much shorter biological half-life of $<$24 h.[5] In the clinical setting, amiodarone proved to be more effective in AF recurrence prevention than dronedarone.[5]

In this study, we investigated the complex effects of these drugs evaluated in an *in-silico* model of human atrial electrophysiology. We hypothesized that (i) the mode of action for amiodarone and dronedarone differs particularly with respect to temporal variations in drug concentration (due to different pharmacokinetics) and heart rate and (ii) the effects differ for different atrial substrates.

Besides a control model, the drug effects were investigated in a substrate representing cAF-induced remodelling and in two human ether-à-go-go-related gene (hERG) mutations (L532P and N588K) as models of familial AF.

Methods

Modelling different substrates

The Courtemanche–Ramirez–Nattel (CRN) model of human atrial myocytes[6] was used to model cellular electrophysiology in the physiological case ('Control'). To investigate the influence of the pharmacological agents on different substrates, the model was adapted.

Chronic AF-induced remodelling was represented by altering the maximum conductance of a subset of the ionic currents based on values extracted from the literature as described before (A. Loewe, M. Wilhelms, O. Dössel, G. Seemann, submitted). In brief, the maximum conductance of the transient outward potassium current I_{to} was reduced by 65%, that of the inward rectifier potassium current I_{K1}, and the slow delayed rectifier potassium current I_{Ks} was increased by 100%, that of the ultra-rapid delayed rectifier potassium current I_{Kur} was reduced by 50%, and that of the L-type calcium current $I_{Ca,L}$ was reduced by 55%. Additionally, the maximum current of the sodium calcium exchanger $I_{Na,Ca}$ was increased by 60%, and that of the sarcoplasmic leak current $I_{up,leak}$ was increased by 50%. The cell capacitance was increased by 20% and the monodomain conductance σ was left unaltered in tissue simulations.

To model the two hERG mutations L532P and N588K, the formulation of I_{Kr} was changed as described before.[7] In brief, 10 parameters were tuned to match measurement data of L532P mutants[8] using a hybrid optimization approach.[9] For N588K, half activation and half inactivation voltages, as well as the slope of the corresponding Boltzmann functions and the time constants of the gate, were adjusted according to data published by McPate *et al.*[10] The altered I_{Kr} formulation represented myocytes being homozygous for the mutations with their characteristic behaviour: premature activation for L532P and delayed inactivation for N588K. Heterozygous expression was approximated by adding an additional I_{Kr} current with unaltered parameters to the model and by reducing the maximum conductance of both I_{Kr} formulations to 50%. In this way, a 1 : 1 mutant to wild-type ratio was assumed.

Modelling the effect of amiodarone and dronedarone

To account for the impact of the pharmacological agents amiodarone and dronedarone, the maximum conductance of the cardiac ion currents was reduced according to the Hill equation: $\theta = [1 + (IC_{50}/D)^{nH}]^{-1}$ with θ being the degree of channel blockade ranging from 0 to 1, IC_{50} being the half-maximal inhibitory concentration, D being the free drug concentration, and nH being the Hill coefficient.

The respective IC_{50} and nH values were extracted from the literature (*Table 1*). For amiodarone, I_{Kr},[11] I_{Ks},[12] I_{Na},[13] $I_{Ca,L}$,[14] I_{NaCa},[15] and I_{NaK}[16] were affected. For dronedarone, I_{Kr},[17] I_{Ks},[18] I_{Na},[13] $I_{Ca,L}$,[19] and I_{Kur}[20] were affected. The resulting Hill curves describing the level of inhibition are shown in *Figure S1* in the Supplementary online material.

The steady-state plasma concentration of amiodarone is reported to range between 1 and 2 μg/mL,[21] corresponding to 1.55–3.11 μM. The therapeutic concentration of dronedarone is reported to be between 84 and 147 ng/mL,[22] corresponding to 0.15–0.26 μM. The effect of the pharmacological agents was modelled for 15 logarithmically spaced free drug concentrations ranging from 0.23 to 23.0 μM for amiodarone and from 0.021 to 2.1 μM for dronedarone.

Restitution in one-dimensional tissue strand

Excitation propagation was simulated in a one-dimensional (1D) tissue strand using the monodomain model. The size of the strand was 20 × 0.1 × 0.1 mm^3. The electrophysiological characteristics under the influence of the drugs were analysed at 20 different basic cycle lengths (BCLs), distributed linearly in the frequency domain ranging from 200 to 1300 ms. To compensate for oscillations of the ion concentrations due to different steady-states for different drug concentrations and BCLs, the system was initialized for 50 beats in a single-cell environment followed by 5 beats in the tissue strand.

Table 1 Pharmacological inhibition of cardiac ion channels

	Amiodarone			Dronedarone		
	IC_{50} (μM)	nH	Source	IC_{50} (μM)	nH	Source
I_{Kr}	2.80	0.91	(12)	0.0591	0.80	(18)
I_{Kur}	–	–		1.00	1.00	(21)
I_{Ks}	3.84	0.63	(13)	5.60	0.51	(19)
I_{Na}	4.84	0.76	(14)	0.54	2.03	(14)
$I_{Ca,L}$	5.80	1.00	(15)	0.83	2.75	(20)
I_{NaCa}	3.30	1.00	(16)	–	–	
I_{NaK}	15.60	1.00	(17)	–	–	

Half maximal inhibitory concentrations (IC_{50}) and Hill coefficients (nH) for amiodarone and dronedarone extracted from the literature.

Restitution curves were calculated as described before.[23] The markers AP duration (APD) at 50% (APD_{50}) and 90% (APD_{90}) repolarization and its slope with respect to the diastolic interval ($dAPD_{90}/dDI$), AP amplitude, maximum diastolic potential (MDP), conduction velocity (CV), effective refractory phase (ERP), wave length (WL), triangulation index (TI), and temporal vulnerable window (VW) were obtained. The diastolic interval (DI) was determined as the difference of BCL and APD_{90}. The TI as a measure for the linearity of the repolarization phase being associated with early afterdepolarizations[24] was defined as $(-V_{m,APD90/2}/(V_{m,Notch} - MDP) - 1)*2$ with $V_{m,APD90/2}$ being the value of the transmembrane voltage (V_m) after half of APD_{90} had passed and $V_{m,Notch}$ being V_m at the first time step after the upstroke for which the absolute value of the slope dV_m/dt was <0.4 V/s. If this condition was not fulfilled within the first 50 ms after the upstroke, the maximum of V_m was considered. For the determination of the VW, a premature stimulus was applied at the centre of the strand after five regular waves had passed from the front of the strand. The duration of the time interval during which the second stimulus induced unidirectional block was defined as the VW.

Furthermore, the resulting AP sequences for each BCL and concentration combination were categorized. Action potentials were considered valid if $V_{m,max}$ exceeded -45 mV and the upstroke velocity exceeded 10 V/s. Decreasing APs were defined as an APD_{90} reduction of $>3\%$ from beat to beat. Furthermore, blockade of all APs, a single AP, or continuous 2 : 1 conduction formed categories. Sequences of valid APs with $>3\%$ variation in APD_{90} were categorized as 'alternans'.

Scoring

To allow for a compact assessment of the evaluated biomarkers, the markers CV, ERP, APD_{50}, $dAPD_{90}/dDI$, TI, VW, and AP category were scored on a continuous scale with one being the best and six being the worst score with respect to arrhythmogeneity. The upper and lower bounds for each marker are shown in *Table* 2. For the evaluation of the trajectories in the BCL-concentration space described below, the individual scores were interpolated bilinearly.

The overall score was determined as the mean of the single scores. If one marker yielded 5.5 or worse or two markers yielded 5 or worse, the overall score 6 was assigned.

Pharmacokinetic scenarios

To assess the biomarkers on a typical trajectory through the two-dimensional BCL-concentration space, pharmacokinetic scenarios with dynamic heart rate variations were defined. For amiodarone, a 200 mg daily dose[3] was administered at 8 am yielding a 20% increase in concentration[25] with respect to the assumed standard concentration of 2.3 μM. For dronedarone, 400 mg doses were administered twice a day[22] at 8 am and 8 pm yielding an assumed increase of 50%. At the time of administration, a reduction of the standard concentration levels by 20 and 50% was defined, respectively. The baseline deviations were modelled using Gaussians. For a second scenario, the drug was assumed to be taken with food resulting in a three-fold increase of the bioavailability for both agents.[5]

The heart rate was assumed to be 70 beats per minute (b.p.m.) (BCL = 857 ms) during the day. Eight episodes of physical stress with an increase of the heart rate up to 120 b.p.m. (BCL = 500 ms) were distributed over the day. From 11 pm to 6 am, the heart rate during sleep was assumed to be 50 b.p.m. (BCL = 1200 ms). For the cAF substrate, the same heart rate course was considered for the sake of comparability. The courses of the heart rate and the drug concentration regarding the two scenarios are shown in the Supplementary online material, *Figures S2* and *S3*.

Table 2 Boundaries for the scoring of biomarkers

	Value for Score 1	Value for Score 6
CV (mm/s)	800	300
$dAPD_{90}/dDI$ (1)	−0.3	1.5
TI (%)	15	95
ERP/ERP_0 (%)	130	60
$APD_{50}/APD_{50,0}$ (%)	130	60
VW/VW_0 (%)	60	130

A continuous score ranging from 1 to 6 was assigned to each biomarker according to the boundary values given in the table. ERP, APD_{50}, and VW were related to the respective values without pharmacological influence (subscript 0). For the AP category, scores were assigned from 1 to 6 as follows: normal, alternans, decreasing AP, single block, 2:1 block, and complete block.

Numerical methods

The ordinary differential equations of the CRN model were solved using the Rush–Larsen scheme for the gating variables and a forward Euler scheme for the remaining variables. The time increment was set to 10 μs. Excitation propagation in tissue was simulated by the parallel modular solver acCELLerate[26] using the monodomain model on a finite difference grid. The grid was composed of cubic voxels with a side length of 0.1 mm. The monodomain conductivity σ was set to an isotropic value of 0.076 S/m yielding a CV of 750 mm/s at a BCL of 1000 ms in the control model.

Results

Dose and frequency response

Using the 1D tissue strand, APs were analysed for different BCLs and drug concentrations. Concentration-induced block could be observed for amiodarone concentrations >23 μM in the cAF substrate, and dronedarone concentrations >1.09 μM in all substrates (see Supplementary material online, *Figure S4*). Frequency-induced block was observed for all substrates but cAF. The BCL below which block was observed decreased with increasing drug concentration resulting in a step-like pattern. The cutoff BCL was higher for dronedarone than for amiodarone.

For non-blocked APs, the biomarkers were analysed on the tissue level with respect to their dose (Supplementary material online, *Figure S5*) and frequency (Supplementary material online, *Figure S6*) response. Below, the results are summarized and quantified for representative BCL and concentration values. Action potential amplitude was decreased for higher concentrations. For the control model and a BCL of 1008 ms, the amplitude decreased from 83.9 mV without any drug to 54.3 mV for 23 μM amiodarone and to 62.1 mV for 1.09 μM dronedarone. Action potential amplitude was almost unaffected by dronedarone concentrations <0.1 μM, whereas an effect could be observed for amiodarone concentrations of ≥ 0.32 μM and higher. For BCLs of ≥ 600 ms, amplitude increased again when the dronedarone concentration was raised from 0.56 to 0.78 μM. In general, lower BCLs were associated with smaller amplitudes. The frequency dependence was markedly decreased in the cAF substrate. For 0.23 μM amiodarone, the difference in amplitude between the lowest and the highest BCL was 3.1 mV for cAF and between 15.4 and 19.9 mV for the other substrates. For 0.021 μM

dronedarone, the difference was 3.8 mV for cAF and between 14.1 and 22.9 mV for the other substrates, respectively.

The dose responses of APD_{50}, APD_{90} and ERP were bell-shaped for amiodarone. For dronedarone, they showed a monotonic increase towards higher concentrations followed by a marked drop beyond a cutoff concentration. The peak amiodarone concentration was between 6.1 and 8.6 μM for control, L532P and N588K, and 3.2 μM for cAF. The amplitude of the APD_{50} bell curve was largest for control (160 ms, +86%), followed by N588K (144 ms, +86%), L532P (117 ms, +96%), and cAF (28 ms, +23%) and showed similar courses for APD_{90} and ERP. For control and N588K, a second smaller peak was observed for an amiodarone concentration of about 1/5 of that of the main peak. The APD_{50}, APD_{90}, and ERP cutoff dronedarone concentrations were between 0.56 and 0.78 μM for all substrates. For the cAF substrate, the drop was not as rapid as for the other substrates. The restitution properties did not differ significantly between substrates and were not markedly altered by varying concentrations of amiodarone and dronedarone. Less pronounced ERP prolongation for lower BCLs is known as reverse use dependence and occurred in the control and N588K substrates for amiodarone (see Supplementary material online, *Figure S7*). For dronedarone, ERP prolongation was decreased for low BCLs in the cAF and L532P substrates—to a lower degree, though. *Figure 1* shows exemplary curves for a BCL of 852 ms (A, B), an amiodarone concentration of 2.3 μM (C), and a dronedarone concentration of 0.21 μM (D), respectively.

The slope of the APD_{90} with respect to the DI showed marked oscillations for concentrations close to cutoff. Towards lower BCLs, the slope increased. This behaviour was most pronounced for the L532P substrate followed by control and N588K. Besides that, no significant dose- or frequency-induced effects were observed.

Conduction velocity was decreased by increased drug concentrations. As was the case for the AP amplitude, the CV was unaffected by dronedarone concentrations <0.1 μM. Inter-substrate variations were marginal: the lowest CVs obtained using amiodarone were 268, 324, 267, and 268 mm/s for control, cAF, L532P, and N588K, respectively. For dronedarone, the values were 417, 505, 414, and

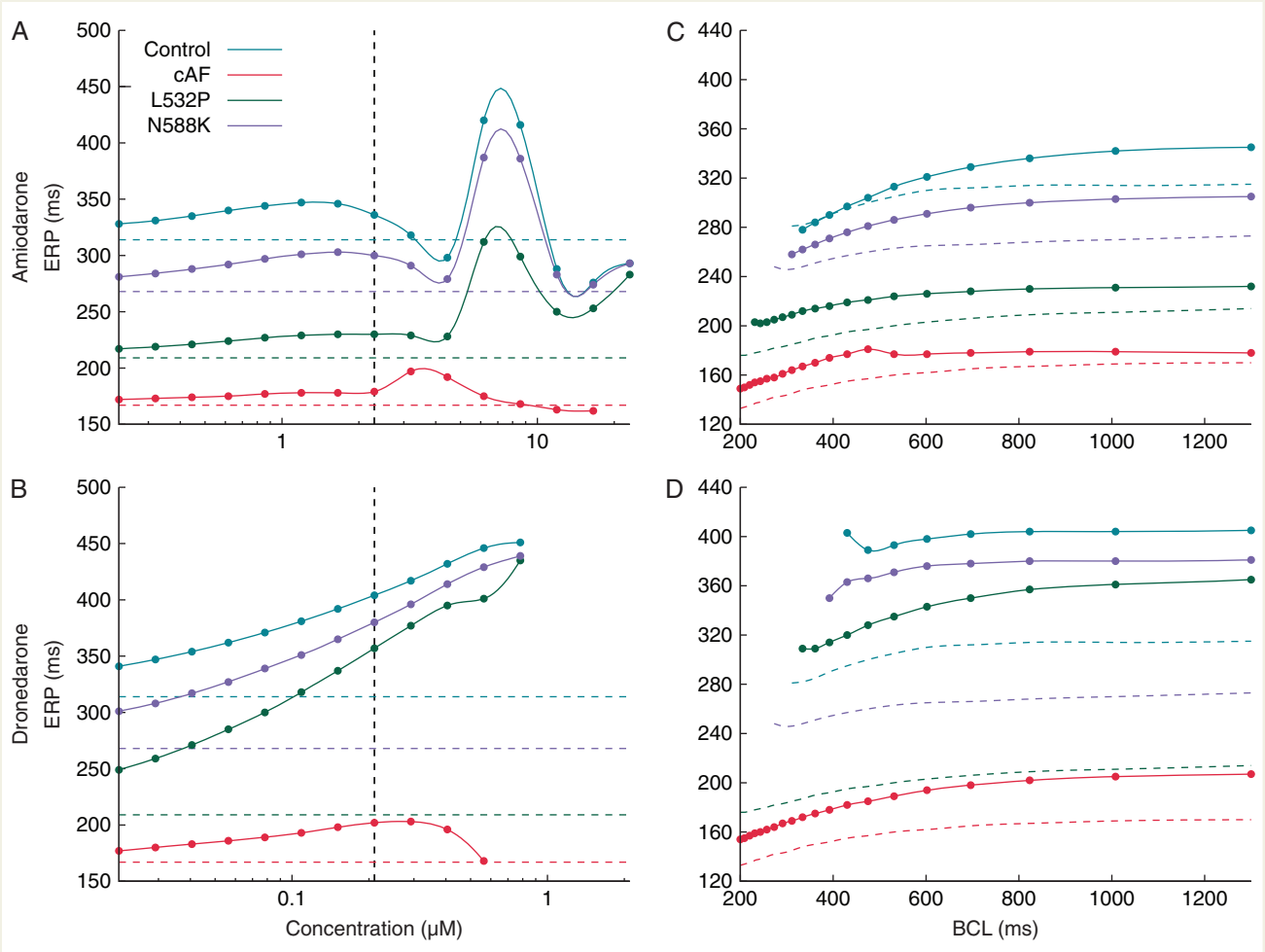

Figure 1 Effective refractory phase for different concentrations of amiodarone (*A*) and dronedarone (*B*) at a BCL of 852 ms. Vertical dashed lines represent the standard concentration of the respective drug, horizontal dashed lines the baseline ERP without drug. Effective refractory phase for different BCLs and 2.3 μM of amiodarone (*C*) or 0.21 μM of dronedarone (*D*). Data points were interpolated using cubic splines.

416 mm/s. For BCLs >500 ms, the CV showed no frequency dependence; for lower BCLs, the CV was decreased. In the cAF substrate, the CV showed no frequency dependence down to BCLs as low as 200 ms.

The MDP showed a tendency towards hyperpolarization for higher amiodarone concentrations. For dronedarone, the tendency was opposite. The amplitude of the change was smaller than 2.5 mV in all cases. For lower BCLs, the MDP was depolarized by up to 4.8, 2.1, 6.1, and 6.2 mV for control, cAF, L532P, and N588K, respectively. The TI exhibited a course qualitatively similar to the ones of the APD markers with a marked drop of the triangulation ~3 μM amiodarone for the cAF substrate and ~6 μM for the other substrates. Outside that region, higher concentrations were associated with an increased TI. For amiodarone concentrations <1 μM, no effect could be observed. Using dronedarone, the TI was decreased for increasing concentrations. However, for the cAF substrate, no change was observed for concentrations up to 0.6 μM. The TI was increased for shorter BCLs.

The temporal VW without drug influence was between 1.5 and 2 ms for the control, L532P, and N588K substrates and vanished with increasing amiodarone concentrations. The initial VW for the cAF substrate was between 0.3 and 0.4 ms. The VW was unaffected by dronedarone for concentrations far from cutoff. Comparing the substrates, all but cAF showed rapid drops of the VW close to the cutoff frequency. As was the case for APD, cAF showed a smoother transition. The VW showed almost no frequency-dependence for BCLs >400 ms. For shorter BCLs, a slight prolongation of the VW was observed. For dronedarone and the L532P substrate, this increase was associated with marked oscillations.

The WL as the product of ERP and CV exhibited a general tendency towards shorter WL for increased amiodarone concentrations. However, the peaks originating from the ERP curves were superimposed on that pattern. These peaks almost restored the WL obtained with zero drug concentration. Dronedarone caused a WL increase for concentrations up to 0.15 μM for cAF and 0.29 μM for all other substrates followed by a significant drop. The WL prolongation compared with zero drug concentration was up to 52 mm (22%) for control, 19 mm (16%) for cAF, 101 mm (64%) for L532P, and 70 mm (34%) for N588K. The frequency response of the WL was dominated by that of the CV.

Scores

Figure 2 shows the resulting total score based on the single scores (see Supplementary material online, *Figure S8*). The drug-free baseline score at a BCL of 1000 ms was 2.33, 2.57, 2.75, and 2.53 for control, cAF, L532P, and N588K, respectively. The CV score yielded higher, thus worse, values for higher concentrations with little frequency and substrate dependence. For BCLs close to cutoff, a slight tendency towards higher scores could be observed. This tendency was more pronounced for dronedarone. The dose dependence was qualitatively similar for dronedarone, although the highest score was 4 for cAF and 5 for all other substrates compared with 6 for amiodarone.

The ERP score dose response for amiodarone showed a bathtub-like shape with minima at 6.17, 3.19, 4.44, and 6.17 μM for control, cAF, L532P, and N588K, respectively. For lower concentrations, a slight tendency towards higher scores could be observed for lower BCLs. For higher concentrations, this behaviour was inverted. For dronedarone, the ERP score decreased with increasing concentrations for all substrates but cAF. cAF dose response showed a minimum at 0.15 μM. For the other substrates, hot spots with high scores could be observed for BCLs close to cutoff for some concentrations. The scores for APD_{50} were qualitatively similar to those for ERP.

$dAPD_{90}/dDI$ scores were dominated by hot spots close to the concentrations associated with ERP score minima for amiodarone and hot spots close to the cutoff BCL for dronedarone. Besides that, a slight tendency towards higher scores for lower BCLs could be observed. The TI scores exhibited marked minima at amiodarone concentrations associated with ERP score minima. Around these concentrations, a tendency towards higher scores could be observed for lower BCLs and higher concentrations resulting in a step-like pattern. For low concentrations in the control substrate, higher BCLs yielded lower scores as well. Scores for dronedarone were consistent with those for ERP. However, the frequency dependence yielding higher scores for lower BCLs was more pronounced for TI than for ERP. The L532P substrate yielded scores as high as 4.9 for small concentrations.

The VW scores showed a general tendency towards lower values for higher amiodarone concentrations. For dronedarone, this tendency was not as pronounced. Hot spots appeared for BCLs close to cutoff for some concentrations of both drugs. For dronedarone in the cAF substrate, hot spots could also be identified for higher BCLs.

Pharmacokinetic scenarios

The courses of the score along the previously defined trajectories in the BCL-concentration space are shown in *Figure 3*. The score for the amiodarone 'food' scenario varied between 1.6 and 2.5 for control, 1.8 and 2.5 for cAF, 2.1 and 2.4 for L532P, and 1.7 and 2.4 for N588K. That for the dronedarone 'food' scenario varied between 1.6 and 5.1 for control, between 1.9 and 6.0 for cAF, between 1.7 and 5.1 for L532P, and between 1.6 and 5.1 for N588K.

For amiodarone, phases of physical stress lead to a reduction of the score during phases of high concentration and an increase of the score during phases of lower concentration with the exception of the cAF substrate for which a stress-induced increase was observed in all phases. In general, the circadian rise of concentration yielded higher scores with the exception of the cAF and the L532P substrate.

For dronedarone, the score peaked above 5 during high concentration, low BCL phases for all substrates in the 'food' scenario. In the scenario in which dronedarone was taken without food, peaks above 2.5 could only be observed in the cAF substrate during low concentration, low BCL phases. In general, the rise in concentration in the 'food' scenario caused an increase of the score. However, for the cAF substrate, the score was lowest during the transition from high to low concentration and vice versa. The circadian concentration variation in the 'non-food' scenario yielded a significant change in the score only for the cAF substrate. A decreasing BCL resulted in higher scores for all substrates.

Discussion

We investigated the effects of amiodarone and dronedarone at different BCLs and drug concentrations in a computational model of

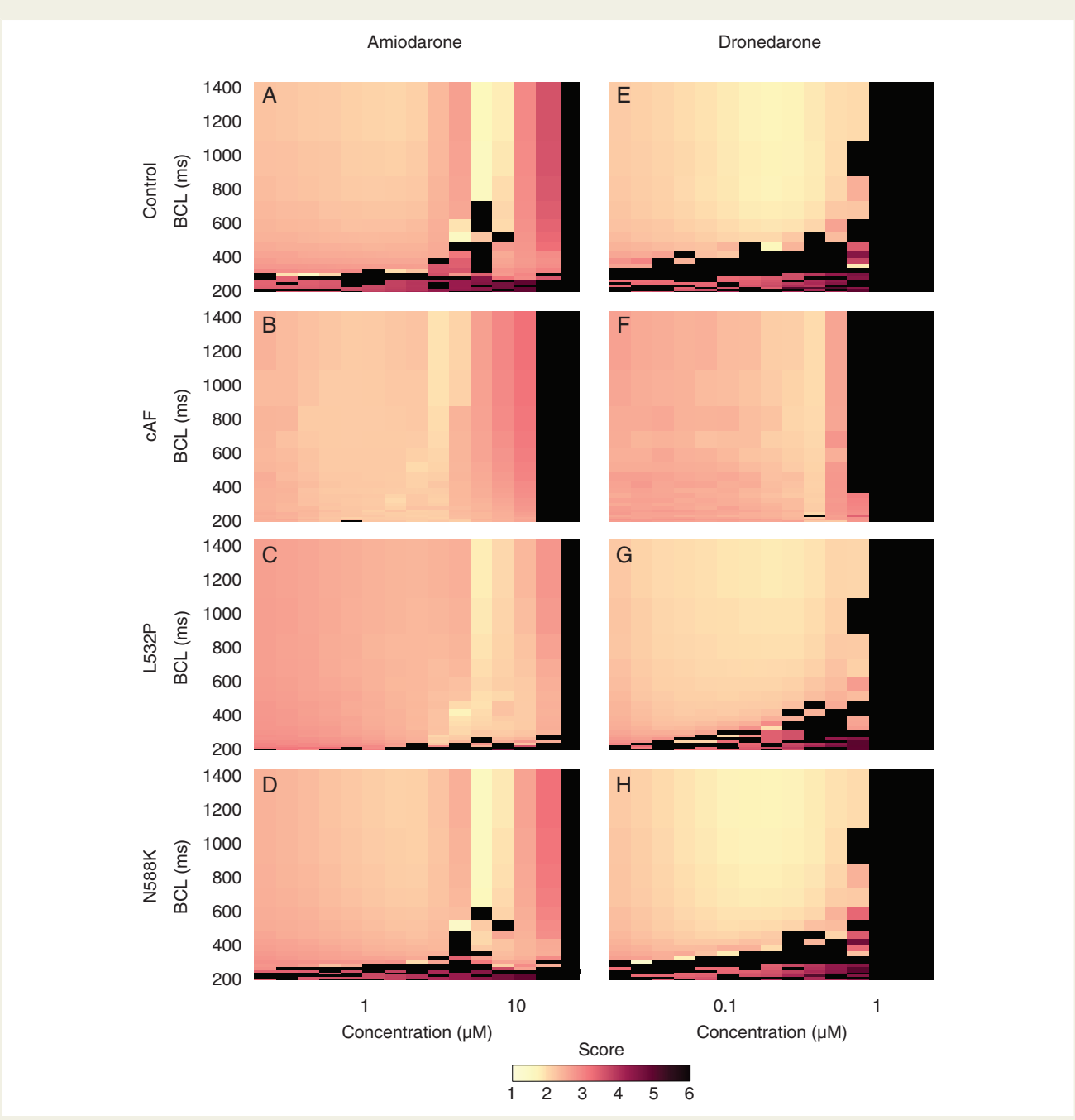

Figure 2 Total score for amiodarone (*A*–*D*) and dronedarone (*E*–*H*) and the four different substrate control (*A* and *E*), cAF-induced remodelling (*B* and *F*), hERG mutation L532P (*C* and *G*), and hERG mutation N588K (*D* and *H*). The scores range from 1 (best) to 6 (worst). The total score was based on the individual scores for CV, $dAPD_{90}/dDI$, TI, ERP/ERP_0, $APD_{50}/APD_{50.0}$, and VW/VW_0. If two markers yielded scores of 5 or worse, or one marker yielded a score of 5.5 or worse, the total score 6 was assigned. Otherwise, the total score was computed as the mean of the marker scores.

human atrial electrophysiology. In addition, the atrial substrate was modified to represent atrial remodelling in chronic AF as well as two mutations associated with familial AF.

Action potential amplitude and CV were associated with the degree of sodium current blockade. Once I_{Na} was reduced by more than 80%, APs could no longer be elicited. As baseline I_{Na} was reduced in the cAF substrate, block occurred for lower concentrations. For low BCLs, the MDP was depolarized due to incomplete repolarization favouring the formation of ectopic beats. Action potential alternans was observed for amiodarone concentrations in the upper range of the 'food' scenario. However, AP alternans was observed for all dronedarone concentrations at BCLs close to cutoff. This characteristic was most pronounced for the control substrate and might be one of the factors explaining the inferior efficacy

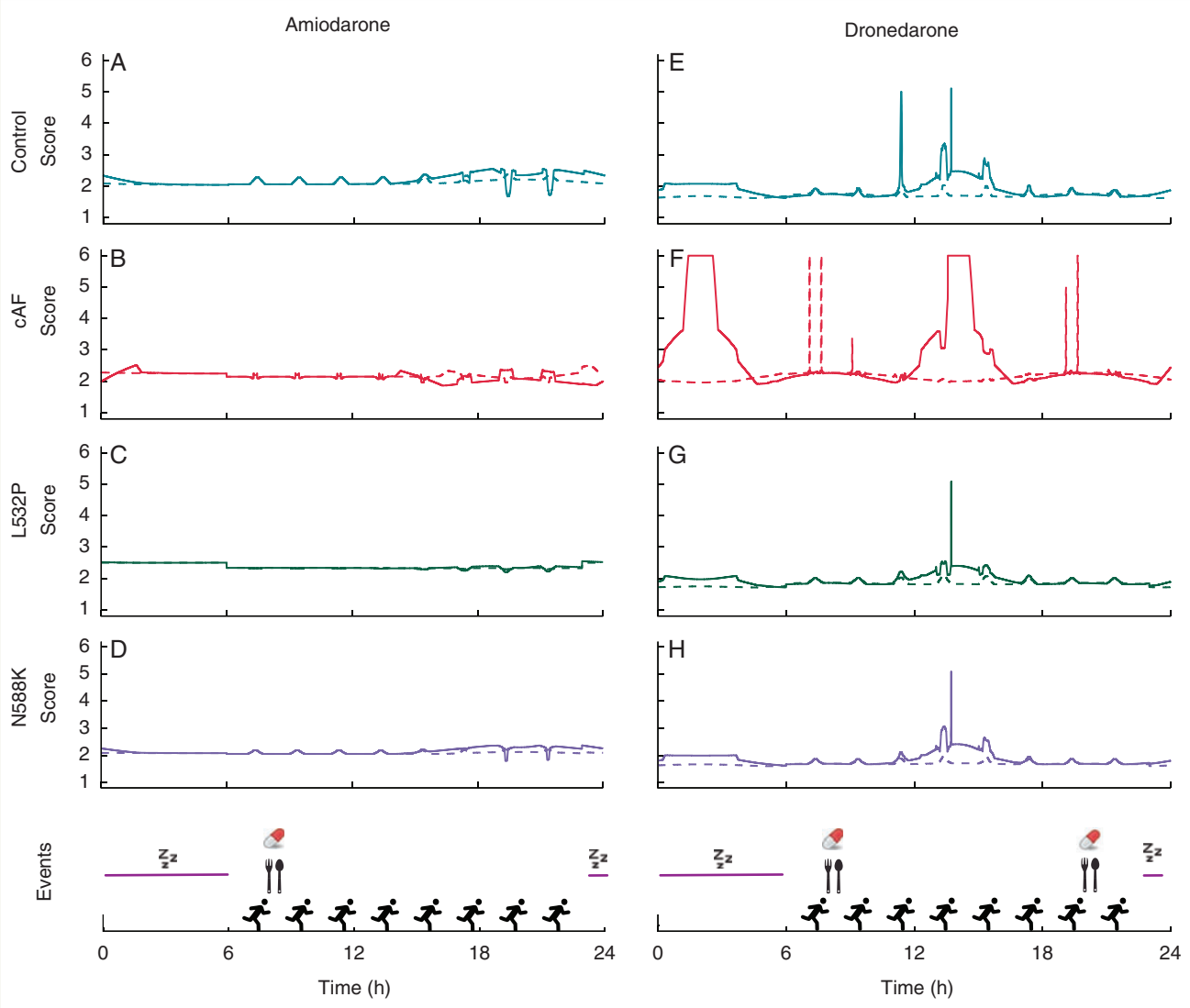

Figure 3 Total score along the trajectories through the BCL-concentration space (see Supplementary material online, *Figures S2* and *S3*). The score was calculated in the same way as for *Figure 2*. The pharmacological agents amiodarone (*A*–*D*) and dronedarone (*E*–*F*) were assumed to be taken with (solid line) or without food (dashed line) resulting in differing bioavailability. The lower panels indicate times of sleep, drug intake and exercise, as well as food intake for the 'food' scenario.

of dronedarone in terms of AF recurrence prevention compared with amiodarone.[27,28]

The amiodarone concentration yielding the lowest score was lower for cAF than for the other substrates. For dronedarone, the opposite was observed. Regarding the circadian course of the score along the trajectories in the BCL-concentration space, amiodarone yielded only minor oscillations. For dronedarone, peaks to critical scores could be observed for all substrates considering the 'food' scenario and for the cAF substrate in both scenarios providing a second indication for inferior efficacy.

Acceleration of the heart rate caused critical scores for some dronedarone concentrations. Interestingly, the score was improved by BCL decrease for some amiodarone concentrations in all but the cAF substrate. Reverse use dependence was observed in the control and N588K substrates for amiodarone, while it occurred only in the other two substrates for dronedarone.

On the whole, the drugs showed markedly different effects in the cAF substrate. The drop of APD, ERP, and VW for high concentrations was not as pronounced as for the other substrates and the VW was shorter. In contrast to the other substrates, the ERP score was not decreased by higher dronedarone concentrations for cAF. These differences resulted in peaks to critical scores in the cAF substrate even for the scenario considering smaller concentration changes.

Previous studies[29–32] investigated the effect of hypothetic and existing Class III antiarrhythmic agents on ventricular electrophysiology using computational models. The focus was drug safety with respect to torsades de pointes. However, there are only few studies

assessing atrial electrophysiology. Tsujimae *et al.*[33] modelled voltage and time-dependent I_{Kr} inhibition caused by dofetilide, vesnarinone, and quinidine. In the work by Wilhelms,[31] I_{Na} blockade was proposed as the reason for amiodarone-induced rotor termination which might be addressed by future research on the 2D tissue level. In the work by Scholz *et al.*,[34] the effect of I_{Kur} inhibitor kinetic properties on rotor termination was investigated. In the work by Aslanidi *et al.*,[35] the change of APD_{90} restitution induced by dronedarone was assessed. The present study is, to the best of our knowledge, the first to create a comprehensive, substrate-specific model of atrial myocytes under the influence of amiodarone and dronedarone.

Shinagawa *et al.*[36] investigated the effect of chronic amiodarone administration in healthy and atrially tachypaced dogs. They described an ERP prolongation due to amiodarone in the healthy dogs, which was also reproduced in this study. However, the restoration of ERP and ERP rate adaptation in tachypaced dogs could not be reproduced. A reason might be the different effects of amiodarone under acute and chronic administration. Moreover, a CV reduction of ~200 mm/s without significant rate dependence was observed,[36] which could be reproduced for an amiodarone concentration of 4.4 μM. In the work by Sun *et al.*,[37] acute *in-vitro* superfusion with either 10 μM dronedarone or 10 μM amiodarone caused a similar reduction of APD_{90} without change of frequency dependence in rabbit muscle preparations. This behaviour could not be reproduced in the present study. However, these quantitatively similar effects for both drugs cannot be explained by the IC_{50} and nH values found in the literature. In guinea pigs, dronedarone did not alter MDP significantly[18] as was the case in this study.

Shinagawa *et al.*[36] reported regionally heterogeneous effects of amiodarone which could be integrated in a heterogeneous model of atrial electrophysiology[38] when appropriate pharmacodynamics data on the ion channel level are available.

Limitations

This study builds on drug–receptor interaction data from the literature. For some cardiac ion currents, the published data are equivocal. Dose-response curves obtained from the same species under comparable conditions for all currents would be desirable to minimize uncertainty as pointed out before.[39] The Hill equation used in this study incorporates neither voltage- or state-dependent block which has been described for some currents,[33,40,41] nor the non-competitive anti-β-adrenergic effect of both drugs[41,42] into the model. The model used in this study could be extended to cover β-adrenergic effects as shown in the reference.[43] The available data describing voltage-dependent block were not sufficient to model the effect reliably and the impact of the drugs is mainly mediated by non-voltage-dependent effects. Additionally, it has to be emphasized that the drug models represent acute and not chronic effects. Differences between acute and chronic administration have been observed particularly for amiodarone.[44] The reason might be a modulation of gene expression.[44] However, the available ion channel level measurement data were not sufficient to identify the Hill curve parameters for chronic amiodarone administration.

The results obtained with the *in-silico* model in terms of absolute concentrations do not necessarily correspond to *in-vivo* measurements because in the latter, the free drug concentration is difficult to assess.[45] Both drugs bind extensively to plasma proteins *in-vitro* and only the free drug concentration is pharmacologically active.[46] Although plasma protein binding has been reported equivocally (e.g. 96.3 ± 0.6%,[47] 99.97–99.99%[46] for amiodarone), this uncertainty does not reduce the validity of the results with respect to relative changes in concentration. The biomarkers taken into account for the scoring and the respective boundaries (see *Table 2*) were chosen based on the dynamic range seen in the simulation results and not validated against clinical data. To draw clinically relevant quantitative conclusions from the score, future research has to address boundary choice.

The pharmacokinetic scenarios in this study were based on a very simplistic model and do not claim to represent the exact course of the concentration during the day. Due to the variation of pharmacokinetic parameters reported in the literature, a detailed model has to be questioned. Furthermore, a variation within a certain range was sufficient for the purpose of this study. Because dronedarone kinetics are difficult to assess *in-vivo*, no data for circadian concentration changes in humans were available. The amplitude was assumed to be 50% of the baseline value due to the shorter elimination half-time compared with amiodarone.[5]

Conclusion

Our findings show how the antiarrhythmic agents amiodarone and dronedarone differentially affect atrial electrophysiology in a concentration- and heart rate-dependent manner. Our results provide possible explanations for the different clinical efficacy of amiodarone and dronedarone in the treatment of AF.

The uncovered effects may aid in the design and optimization of patient group-specific pharmacotherapy considering the atrial substrate.

Supplementary material

Supplementary material is available at *Europace* online.

Acknowledgements

The icons in *Figure 3* were designed by Flaticon.com.

Conflict of interest: none declared.

Funding

This work was supported by Deutsche Forschungsgemeinschaft (grant number DFG SE 1758/3-1 to M.W. and G.S., grant number DFG SCHO 1350/2-1 to E.S.).

References

1. Wijffels MC, Kirchhof CJ, Dorland R, Allessie MA. Atrial fibrillation begets atrial fibrillation. A study in awake chronically instrumented goats. *Circulation* 1995;**92**:1954–68.
2. Lubitz SA, Ozcan C, Magnani JW, Kääb S, Benjamin EJ, Ellinor PT. Genetics of atrial fibrillation: implications for future research directions and personalized medicine. *Circ Arrhythm Electrophysiol* 2010;**3**:291–9.
3. Camm AJ, Kirchhof P, Lip GY, Schotten U, Savelieva I, Ernst S *et al.* Guidelines for the management of atrial fibrillation: the Task Force for the Management of Atrial Fibrillation of the European Society of Cardiology (ESC). *Europace* 2010;**12**:1360–420.
4. Page RL, Hamad B, Kirkpatrick P. Dronedarone. *Nat Rev Drug Discov* 2009;**8**:769–70.
5. Kathofer S, Thomas D, Karle CA. The novel antiarrhythmic drug dronedarone: comparison with amiodarone. *Cardiovasc Drug Rev* 2005;**23**:217–30.

6. Courtemanche M, Ramirez RJ, Nattel S. Ionic mechanisms underlying human atrial action potential properties: insights from a mathematical model. *Am J Physiol* 1998; **275**:H301–21.
7. Loewe A, Wilhelms M, Fischer F, Scholz EP, Dossel O, Seemann G. Arrhythmic potency of human ether-à-go-go-related gene mutations L532P and N588 K in a computational model of human atrial myocytes. *Europace* 2014;**16**:435–43.
8. Hassel D, Scholz EP, Trano N, Friedrich O, Just S, Meder B *et al.* Deficient zebrafish ether-à-go-go-related gene channel gating causes short-QT syndrome in zebrafish reggae mutants. *Circulation* 2008;**117**:866–75.
9. Loewe A, Wilhelms M, Fischer F, Scholz EP, Dössel O, Seemann G. Impact of hERG mutations on simulated human atrial action potentials. *Biomed Tech* 2013;**58**(Suppl 1). doi:10.515/bmt-2013-4331.
10. McPate MJ, Duncan RS, Milnes JT, Witchel HJ, Hancox JC. The N588K-HERG K^+ channel mutation in the "short QT syndrome": mechanism of gain-in-function determined at 37°C. *Biochem Biophys Res Commun* 2005;**334**:441–9.
11. Kamiya K, Nishiyama A, Yasui K, Hojo M, Sanguinetti MC, Kodama I. Short- and long-term effects of amiodarone on the two components of cardiac delayed rectifier K^+ current. *Circulation* 2001;**103**:1317–24.
12. Zankov DP, Ding W-G, Matsuura H, Horie M. Open-state unblock characterizes acute inhibition of I_{Ks} potassium current by amiodarone in guinea pig ventricular myocytes. *J Cardiovasc Electrophysiol* 2005;**16**:314–22.
13. Lalevee N, Nargeot J, Barrere-Lemaire S, Gautier P, Richard S. Effects of amiodarone and dronedarone on voltage-dependent sodium current in human cardiomyocytes. *J Cardiovasc Electrophysiol* 2003;**14**:885–90.
14. Nishimura M, Follmer CH, Singer DH. Amiodarone blocks calcium current in single guinea pig ventricular myocytes. *J Pharmacol Exp Ther* 1989;**251**:650–9.
15. Watanabe Y, Kimura J. Acute inhibitory effect of dronedarone, a noniodinated benzofuran analogue of amiodarone, on Na^+/Ca^{2+} exchange current in guinea pig cardiac ventricular myocytes. *Naunyn Schmiedebergs Arch Pharmacol* 2008;**377**: 371–6.
16. Gray DF, Mihailidou AS, Hansen PS, Buhagiar KA, Bewick NL, Rasmussen HH *et al.* Amiodarone inhibits the Na^+-K^+ pump in rabbit cardiac myocytes after acute and chronic treatment. *J Pharmacol Exp Ther* 1998;**284**:75–82.
17. Ridley JM, Milnes JT, Witchel HJ, Hancox JC. High affinity HERG K^+ channel blockade by the antiarrhythmic agent dronedarone: resistance to mutations of the S6 residues Y652 and F656. *Biochem Biophys Res Commun* 2004;**325**:883–91.
18. Gautier P, Guillemare E, Marion A, Bertrand J-P, Tourneur Y, Nisato D. Electrophysiologic characterization of dronedarone in guinea pig ventricular cells. *J Cardiovasc Pharmacol* 2003;**41**:191–202.
19. Bogdan R, Goegelein H, Ruetten H. Effect of dronedarone on Na^+, Ca^{2+} and HCN channels. *Naunyn-Schmied Arch Pharmacol* 2011;**383**:347–56.
20. Gautier P, Guillemare E, Djandjighian L, Marion A, Planchenault J, Bernhart C *et al.* In vivo and in vitro characterization of the novel antiarrhythmic agent SSR149744C: electrophysiological, anti-adrenergic, and anti-angiotensin II effects. *J Cardiovasc Pharmacol* 2004;**44**:244–57.
21. Podrid PJ. Amiodarone: reevaluation of an old drug. *Ann Intern Med* 1995;**122**: 689–700.
22. Sanofi-Aventis Canada Inc. Product Monograph MULTAQ, Dronedarone Tablets. Laval, Quebec H7L 4A8, 2011.
23. Wilhelms M, Hettmann H, Maleckar MMC, Koivumäki JT, Dössel O, Seemann G. Benchmarking electrophysiological models of human atrial myocytes. *Front Physiol* 2013;**3**:1–16.
24. Hondeghem LM, Carlsson L, Duker G. Instability and triangulation of the action potential predict serious proarrhythmia, but action potential duration prolongation is antiarrhythmic. *Circulation* 2001;**103**:2004–13.
25. Haffajee CI, Love JC, Canada AT, Lesko LJ, Asdourian G, Alpert JS. Clinical pharmacokinetics and efficacy of amiodarone for refractory tachyarrhythmias. *Circulation* 1983;**67**:1347–55.
26. Seemann G, Sachse FB, Karl M, Weiss DL, Heuveline V, Dössel O. Framework for modular, flexible and efficient solving the cardiac bidomain equation using PETSc. *Math Ind* 2010;**15**:363–9.
27. Narayan SM, Bode F, Karasik PL, Franz MR. Alternans of atrial action potential during atrial flutter as a percursor to atrial fibrillation. *Circulation* 2002;**106**:1968–73.
28. Gong Y, Xie F, Stein KM, Garfinkel A, Culianu CA, Lerman BB *et al.* Mechanism underlying initiation of paroxysmal atrial flutter/atrial fibrillation by ectopic foci: a simulation study. *Circulation* 2007;**115**:2094–102.
29. Zemzemi N, Bernabeu MO, Saiz J, Cooper J, Pathmanathan P, Mirams GR *et al.* Computational assessment of drug-induced effects on the electrocardiogram: from ion channel to body surface potentials. *Br J Pharmacol* 2013;**168**:718–33.
30. Wilhelms M, Holl LP, Dössel O, Seemann G. Impact of antiarrhythmic drugs on a virtual model of atrial fibrillation. *Biomed Tech/Biomed Eng* 2012;**57**(Suppl 1). doi:10.515/bmt-2012-4196.
31. Wilhelms M. *Multiscale modeling of cardiac electrophysiology: adaptation to atrial and ventricular rhythm disorders and pharmacological treatment. Karlsruhe Transactions on Biomedical Engineering*; 20. Karlsruhe: KIT Scientific Publishing, 2013.
32. Obiol-Pardo C, Gomis-Tena J, Sanz F, Saiz J, Pastor M. A multiscale simulation system for the prediction of drug-induced cardiotoxicity. *J Chem Inf Model* American Chemical Society; 2011;**51**:483–92.
33. Tsujimae K, Suzuki S, Murakami S, Kurachi Y. Frequency-dependent effects of various IKr blockers on cardiac action potential duration in a human atrial model. *Am J Physiol Heart Circ Physiol* 2007;**293**:H660–9.
34. Scholz EP, Carrillo-Bustamante P, Fischer F, Wilhelms M, Zitron E, Dössel O *et al.* Rotor termination is critically dependent on kinetic properties of I_{Kur} inhibitors in an *in-silico* model of chronic atrial fibrillation. *PLoS One* 2013;**8**:e83179.
35. Aslanidi OV, Al-Owais M, Benson AP, Colman M, Garratt CJ, Gilbert SH *et al.* Virtual tissue engineering of the human atrium: modelling pharmacological actions on atrial arrhythmogenesis. *Eur J Pharm Sci* 2011;**46**:209–21.
36. Shinagawa K. Effects of antiarrhythmic drugs on fibrillation in the remodeled atrium: insights into the mechanism of the superior efficacy of amiodarone. *Circulation* 2003; **107**:1440–6.
37. Sun W, Sarma JSM, Singh BN. Chronic and acute effects of dronedarone on the action potential of rabbit atrial muscle preparations: comparison with amiodarone. *J Cardiovasc Pharmacol* 2002;**39**:677–84.
38. Krueger MW, Dorn A, Keller DUJ, Holmqvist F, Carlson J, Platonov PG *et al. In-silico* modeling of atrial repolarization in normal and atrial fibrillation remodeled state. *Med Biol Eng Comput* 2013;**51**:1105–19.
39. Mirams GR, Davies MR, Cui Y, Kohl P, Noble D. Application of cardiac electrophysiology simulations to pro-arrhythmic safety testing. *Br J Pharmacol* 2012;**167**:932–45.
40. Kodama I, Nikmaram MR, Boyett MR, Suzuki R, Honjo H, Owen JM. Regional differences in the role of the Ca^{2+} and Na^+ currents in pacemaker activity in the sinoatrial node. *Am J Physiol* 1997;**272**:H2793–806.
41. Patel C, Yan GX, Kowey PR. Dronedarone. *Circulation* 2009;**120**:636–44.
42. Kodama I, Kamiya K, Toyama J. Cellular electropharmacology of amiodarone. *Cardiovasc Res* 1997;**35**:13–29.
43. Keller DUJ, Bohn A, Dössel O, Seemann G. *In-silico* evaluation of beta-adrenergic effects on the long-QT syndrome. *Proc Comput Cardiol* 2010;**2010**:825–8.
44. Kodama I, Kamiya K, Toyama J. Amiodarone: ionic and cellular mechanisms of action of the most promising class III agent. *Am J Cardiol* 1999;**84**:20r–8r.
45. Xie C, Yang S, Zhong D, Dai X, Chen X. Simultaneous determination of dronedarone and its active metabolite debutyldronedarone in human plasma by liquid chromatography-tandem mass spectrometry: application to a pharmacokinetic study. *J Chromatogr B Analyt Technol Biomed Life Sci* 2011;**879**:3071–5.
46. Veronese ME, McLean S, Hendriks R. Plasma protein binding of amiodarone in a patient population: measurement by erythrocyte partitioning and a novel glass-binding method. *Br J Clin Pharmacol* 1988;**26**:721–31.
47. Latini R, Tognoni G, Kates RE. Clinical pharmacokinetics of amiodarone. *Clin Pharmacokinet* 1984;**9**:136–56.